

A preference for Dynamical Dark Energy?

David Benisty^{1, 2, 3, *} and Denitsa Staicova^{4, †}

¹DAMTP, Centre for Mathematical Sciences, University of Cambridge, Wilberforce Road, Cambridge CB3 0WA, United Kingdom

²Physics Department, Ben-Gurion University of the Negev, Beer-Sheva 84105, Israel

³Frankfurt Institute for Advanced Studies (FIAS), Ruth-Moufang-Strasse 1, 60438 Frankfurt am Main, Germany

⁴Institute for Nuclear Research and Nuclear Energy, Bulgarian Academy of Sciences, Sofia, Bulgaria

Dynamical Dark Energy (DDE) is a possible solution to the Hubble tension. This work analyses the combination of Baryon Acoustic Oscillation (BAO) data that include 19 points from the range $0.11 \leq z \leq 2.40$ and additional points from the Cosmic Microwave Background (CMB) Distant Priors. We test equation of states with a Linear, CPL and a Logarithm dependence on the redshift. DDE seems to be stronger than the standard Λ CDM model statistically using different selection criteria. The result calls for new observations and stimulates the investigation of alternative theoretical models beyond the standard model. We also test the same dataset on the Ω_k CDM model but for it, Λ CDM gives better statistical measures.

INTRODUCTION

The Hubble constant H_0 measures the current expansion rate of the Universe [1, 2]. An estimation of H_0 from direct measurements from the late universe [3–7] yields $H_0 = 73.2 \pm 1.3 \text{ km/sec/Mpc}$. Other method uses the measurements of temperature and polarization anisotropies in the Cosmic Microwave Background (CMB), in combination with low-redshift probes of the expansion history, such as Baryon Acoustic Oscillation (BAO) or SNeIa distance measurements [8–15] with $H_0 = 67.27 \pm 0.66 \text{ km s}^{-1} \text{ Mpc}^{-1}$. The discrepancy between the H_0 measurements is one of the fundamental problems in cosmology [16–20]. The question whether the dark energy is a constant energy density or with a dynamical behavior is modeled in different theories [18, 21? –25]. This motivates a host of Dynamical Dark Energy (DDE) parametrisations [26–28] in order to search for deviations from Λ in observational data. The DDE also may resolve the Hubble tension, particularly for the Early Dark Energy models [29–32]. This letter combines the CMB (distant priors) and the BAO measurements to present a preference for some DDE model.

THEORY

A Friedmann-Lemaître-Robertson-Walker metric with the scale parameter $a = 1/(1+z)$ is considered, where z is the redshift. The evolution of the universe for it is governed by the Friedmann equation which connects the equation of state for Λ CDM background:

$$E(z)^2 = \Omega_r(1+z)^4 + \Omega_m(1+z)^3 + \Omega_k(1+z)^2 + \Omega_\Lambda(z), \quad (1)$$

with the expansion of the universe $E(z)^2 = H(z)/H_0$, where $H(z) := \dot{a}/a$ is the Hubble parameter at redshift z and H_0 is the Hubble parameter today. Ω_r , Ω_m , Ω_Λ and Ω_k are the fractional densities of radiation, matter, dark energy and the spatial curvature at redshift $z = 0$. Even

though the radiation density at the redshifts probed by BAO is negligible, we include it as $\Omega_r = 1 - \Omega_m - \Omega_\Lambda - \Omega_k$. The spatial curvature is expected to be zero for a flat Universe, $\Omega_k = 0$. We can expand this simple model by considering a dark energy component depending on z . This can be done with a generalization of the Chevallier-Polarski-Linder (CPL) parametrization [33–35]:

$$\Omega_\Lambda(z) = \Omega_\Lambda^{(0)} \exp \left[\int_0^z \frac{3(1+w(z'))dz'}{1+z'} \right] \quad (2)$$

in which we consider three possible models:

$$w(z) = \begin{cases} w_0 + w_a z & \text{Linear} \\ w_0 + w_a \frac{z}{z+1} & \text{CPL} \\ w_0 - w_a \log(z+1) & \text{Log} \end{cases} \quad (3)$$

which recover Λ CDM for $w_0 = -1, w_a = 0$.

The distance priors provide effective information of CMB power spectrum in two aspects: the acoustic scale l_A characterizes the CMB temperature power spectrum in the transverse direction, leading to the variation of the peak spacing, and the "shift parameter" R influences the CMB temperature spectrum along the line-of-sight direction, affecting the heights of the peaks. The popular definitions of the distance priors are [36]:

$$l_A = (1+z_*) \frac{\pi D_A(z_*)}{r_s(z_*)}, \quad R \equiv (1+z_*) \frac{D_A(z_*) \sqrt{\Omega_m} H_0}{c}, \quad (4)$$

where z_* is the redshift at the photon decoupling epoch. Here we use the values of $z_* \approx 1089$ given by the *Planck* 2018 chains. r_s is the comoving sound horizon. The angular diameter distance D_A is given by

$$D_A = \frac{c}{(1+z)H_0 \sqrt{|\Omega_k|}} \text{sinn} \left[|\Omega_k|^{1/2} \int_0^z \frac{dz'}{E(z')} \right], \quad (5)$$

where $\text{sinn}(x) \equiv \sin(x), x, \sinh(x)$ for $\Omega_k < 0, \Omega_k = 0, \Omega_k > 0$ respectively. [37] derives the distance priors in

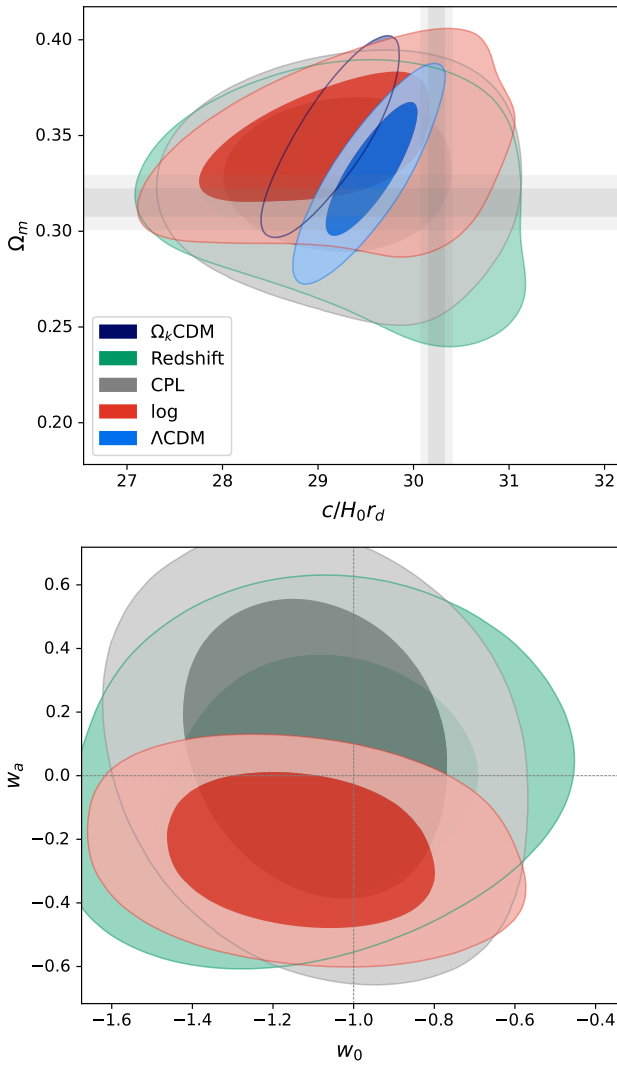


FIG. 1. The 2D contour plot of $c/(H_0 r_d)$, Ω_m and Ω_Λ with different parametrization of DDE. The upper panel shows the results for Ω_m vs. $c/(H_0 r_d)$ and the lower panel shows the results for w and w_a . Λ CDM corresponds to $w_0 = -1$ and $w_a = 0$ which is outside the distributions and give strong sign for DDE. The grey lines show the 1σ and 2σ of Ω_m and $c/(H_0 r_d)$ as measured by Planck 2018, while on the bottom plot the gray cross shows where we recover Λ CDM.

several different models using *Planck* 2018 TT,TE,EE + lowE which is the latest CMB data from the final full-mission *Planck* measurement [15].

METHOD

The dataset we are using is a collection of points from different BAO observations [13, 38–49], to which we add the CMB distant prior [50]. We use a Monte Carlo Markov Chain (MCMC) nested sampler to find the best fit. Concretely, we use the open-source package

PolyChord [51] with the *GetDist* package [52] to present the results. Furthermore, we use *mpmath* to increase the digits of precision to 32. The prior is a uniform distribution for all the quantities: $\Omega_m \in [0.; 1.]$, $\Omega_\Lambda \in [0.; 1 - \Omega_m]$, $\Omega_r \in [0.; 1 - \Omega_m - \Omega_\Lambda]$, $c/(H_0 r_d) \in [25; 35]$, $w_0 \in [-1.5; -0.5]$ and $w_a \in [-0.5; 0.5]$. Since the distance prior is defined at the decoupling epoch (z_*) and the BAO – at drag epoch (z_d), we parametrize the difference between $r_s(z_*)$ and $r_s(z_d)$ as $r_* = r_d \times rat$, where the prior for the ratio is $rat \in [0.9; 1.1]$. For testing the Ω_k model we use as a prior $\Omega_k \in [-0.1, 0.1]$. The priors of the other parameters are $c/(H_0 r_d) \in (25, 35)$, $\Omega_m \in [0.2, 1 - \Omega_k]$, $\Omega_\Lambda \in [0, 1 - \Omega_m - \Omega_k]$, $r_d/r_s \in [0.9, 1.1]$.

To avoid the possible correlations in the BAO dataset, we use the methodology in [53, 54]. This method avoids the use of N-body mocks to find the covariance matrices due to systematic errors and replaces it with an evaluation of the effect of possible small correlation on the final result. The covariance matrix for uncorrelated points is: $C_{ii} = \sigma_i^2$. Since we're trying to simulate correlations, we introduce a number of randomly selected nondiagonal elements in the covariance matrix while keeping it symmetric. The positions of the non-diagonal elements are chosen randomly and the magnitude of those randomly selected covariance matrix element C_{ij} is set to $C_{ij} = 0.5\sigma_i\sigma_j$, where $\sigma_i\sigma_j$ are the published 1σ errors of the data points i, j . We introduce positive correlations in up to 6 pairs of randomly selected data points (more than 25% of the data). The figures in the appendix show the cornerplots with different randomized points for all the models we employ in this article. The best fit values of the corresponding $c/(H_0 r_d)$, Ω_m and Ω_Λ are shown in the table below. The mean values as well as the errors are not affected significantly from adding a random covariance inside which indicates that we can consider the chosen set of BAO points for effectively uncorrelated. This means that even if there exists a correlation between them in the chosen limit, it wouldn't change the presented results significantly. Furthermore, we see that while using a model with larger number of inferred parameters increases the errors, the difference in the mean values remains below 10% on average.

RESULTS

Table I and Fig. 1 shows the final values obtained by running MCMC on the selected priors. All the models give very similar values for the physical quantities $c/(H_0 r_d)$, Ω_m and Ω_Λ , despite the very wide prior imposed on Ω_m . This comes in contrast with our previous study [54] where the inferred value of Ω_m was very sensitive to the result for r_d . Since in the present work we avoid the degeneracy between r_d and H_0 by considering the combined quantity $c/(H_0 r_d)$ this leads to a very strict limit on Ω_m . From the table it is clear that the

Model	$c/(H_0 r_d)$	Ω_m	Ω_Λ	Ω_K	w_0	w_a
ΛCDM	29.6 ± 0.3	0.331 ± 0.02	0.668 ± 0.019	0.000	-1.000	0
Linear	29.1 ± 0.8	0.344 ± 0.019	0.655 ± 0.02	0.000	-1.125 ± 0.231	-0.237 ± 0.166
CPL	29.3 ± 0.8	0.328 ± 0.022	0.671 ± 0.025	0.000	-1.087 ± 0.186	0.079 ± 0.322
Log	29.2 ± 0.8	0.326 ± 0.025	0.673 ± 0.026	0.000	-1.096 ± 0.241	-0.02 ± 0.244
$\Omega_k\text{CDM}$	29.1 ± 0.3	0.349 ± 0.018	0.745 ± 0.018	-0.094 ± 0.003	-1.000	0

TABLE I. The posterior distribution for $c/(H_0 r_d)$, Ω_m , Ω_Λ and w_0, w_a for different parametrization of DDE.

Model	DIC	ΔDIC	BF
ΛCDM	23.4		
Linear	23.1	0.35	1.1
CPL	23.5	-0.05	0.3
Log	23.6	-0.11	0.4
$\Omega_k\text{CDM}$	23.2	0.21	121

TABLE II. *DIC and BF selection criteria for different models compared to the default ΛCDM model.*

Model	Planck 2018	R20 + H0LiCOW
ΛCDM	2.18	0.58
Linear	1.34	0.26
CPL	1.27	0.36
Log	1.23	0.32
$\Omega_k\Lambda\text{CDM}$	4.03	0.31

TABLE III. *The tension between the models and the combined observations.*

current dataset favors $w \leq -1$ and also $\Omega_k < 0$. In all cases the $rat \sim 0.915$ placing the drag horizon at about $r_d = 161\text{Mpc}$ if one assumes $r_* = 146.8\text{Mpc}$ which is about 5% higher than the expected value.

As for $\Omega_k\text{CDM}$ we see that the error on Ω_k seems very strong. According to our observations, if one uses a smaller prior still bracketing the zero (i.e. $[-0.05, 0.005]$), the inferred value for Ω_k will tend to the left (negative) limit. We didn't use that smaller prior as it results in larger reduced χ^2 and also, it implies the assumption of a flat universe.

To compare the different models, we use well-known statistical measures. The results can be seen in Table [2]. When comparing the models, we do not use the standard AIC and BIC measures, since for small datasets, they are dominated by the number of parameters in the model (which are 4 for ΛCDM , 6 for the DE models and 5 for $\Omega_k\text{CDM}$). For this reason, we use deviance information criterion (DIC) and the Bayes Factor (BF) which rely on the numerically evaluated likelihood and evidence, making them more unbiased. The DIC criterion, just like the AIC, selects the best model to be the one with the minimal value of the DIC measurement. The reference table we use for DIC is: $\Delta\text{DIC} > 10$ shows strong support for the model with lower DIC, $\Delta\text{DIC} = 5 - 10$

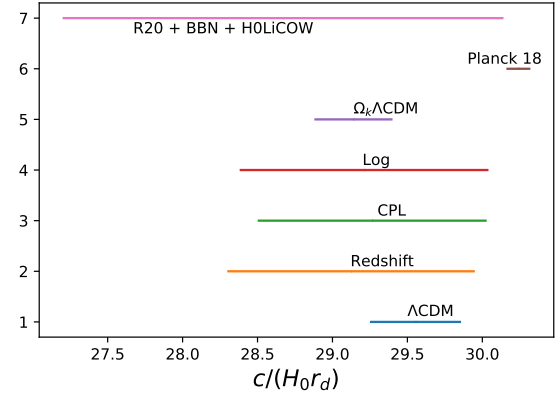


FIG. 2. *The final values of the $c/(H_0 r_d)$ from different DDE models in a comparison with the values from Planck and SH0ES. The color-coding is the same as on previous figures.*

shows substantial support for the model with lower DIC, $\Delta\text{DIC} < 5$ gives ambiguous support for the model with lower DIC. In our case, we have 2 DDE models with DIC smaller than that of ΛCDM , but all of the $|\Delta\text{DIC}| < 5$ (or even 2, which is the limit for AIC), showing that the evidence distinguishing any of the models is very weak. The same applies for $\Omega_k\text{CDM}$.

The Bayes factor, calculated always as the ratio between the evidence of ΛCDM over one of the other models, definitely shows negative support for the ΛCDM model (having $\text{BF}_{1|1}$) compared to the CPL and the Log models. Following Jeffrey's scale [55], the evidence in support of the DDE models is on the limit of substantial (this is the conservative limit, some runs gave strong to very strong support for DDE). The support for $\Omega_k\text{CDM}$ is very weak, signs of which have been seen also elsewhere [54, 56, 57]. Interestingly, the Ω_k value excludes zero at the 95% confidence interval (again due to the very small error on the inferred Ω_k).

The dataset combines the H_0 and the r_d in one quantity. Therefore we estimate the new variable $c/(H_0 r_d) \sim 30$. Fig 2 shows the values of the $c/(H_0 r_d)$ for different models vs. the result from Planck 30.24 ± 0.08 and the combined result of 28.67 ± 1.47 . The tension between these measurements is 1.065σ . Table shows the tensions rate (in number of sigmas) between our fit and these of the early Planck 2018 estimation and the late time esti-

mation from R20 + H0LicoW + BBN. The DDE models reduce the tension with the tension from the Λ CDM model both from the Planck 2018 data and the late time estimation. However we cannot state that a complete solution to the cosmic tension is achieved.

DISCUSSION

This paper is raising the possibility for DDE preference over Λ CDM, using the BAO and the CMB distant priors datasets. From the DIC and the BF comparison seems that there is a strong support for CPL or Log DDE mode over Λ CDM. This is particularly interesting considering the wide priors we use, the fact the DDE models have more parameters and that we have one additional parameter – the ratio between the two sound horizons. DDE models are particularly interesting in connection to modified gravity theories.

Papers have shown possible extensions to the standard model: [58] gives a strong preference for DDE from some earlier BAO dataset. [59] shows that a combined analysis of CMB anisotropy and the luminosity distance data excludes a flat universe. [60, 61] do not detect any significant deviation from GR based on DES and BOSS combined measurements. Combined with our results, there is a possibility for DDE as a viable extension of the standard model and future experiments should shed more light whether it is the best model.

D.B. gratefully acknowledge the support from Frankfurt Institute for Advanced Studies (FIAS) as well the to support from Ben-Gurion University in Beer-Sheva, Israel. D.B. also thanks to the Grants Committee of the Rothschild and the Blavatnik Cambridge Fellowships for generous supports. D.S. is thankful to Bulgarian National Science Fund for support via research grants DN 08-17, DN-18/1, KP-06-N 38/11. We have received partial support from European COST actions CA15117 and CA18108.

* benidav@post.bgu.ac.il

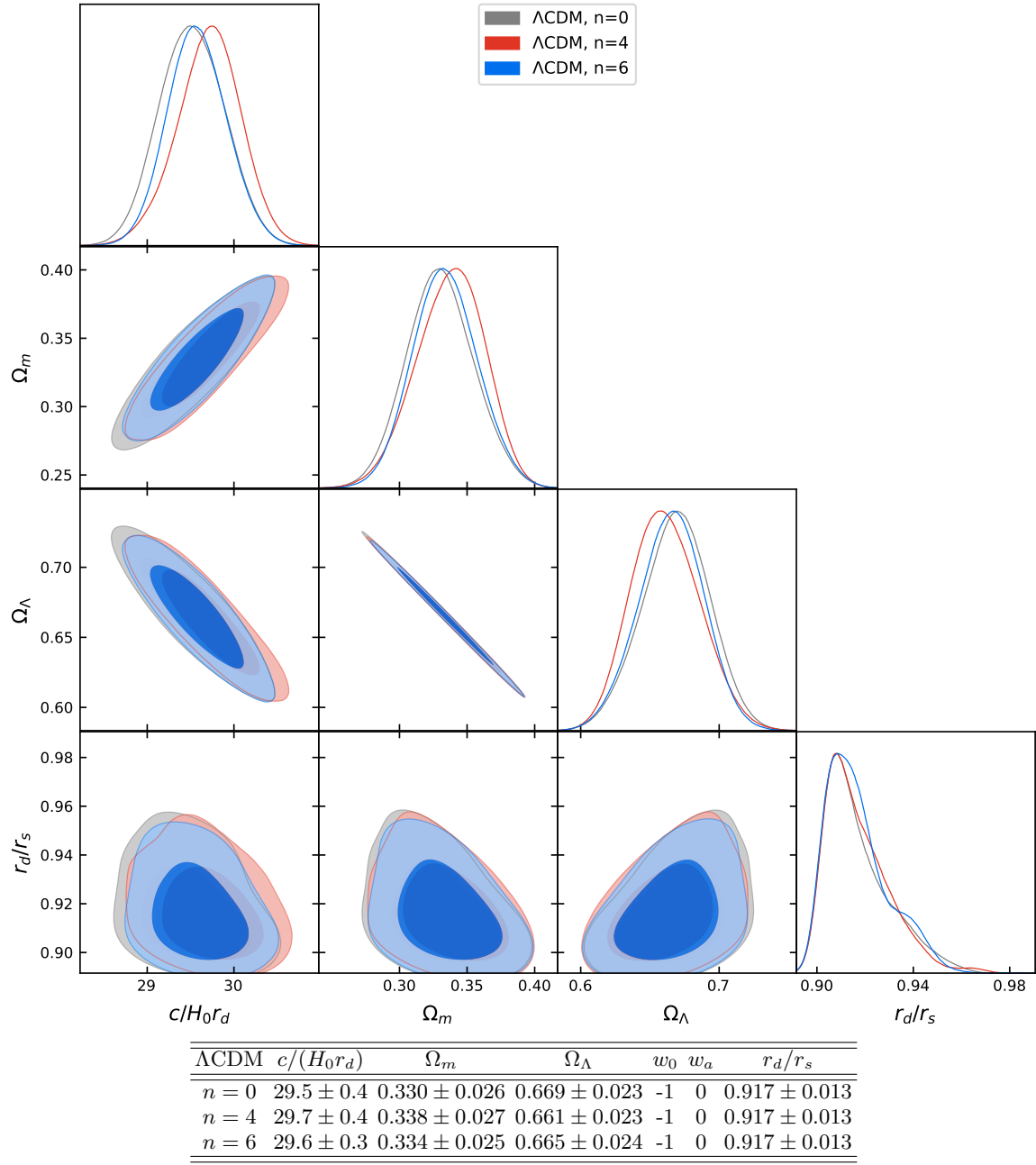
† dstaicova@inrne.bas.bg

- [1] E. Hubble, *Proc. Nat. Acad. Sci.* **15**, 168 (1929).
- [2] W. L. Freedman and B. F. Madore, *Ann. Rev. Astron. Astrophys.* **48**, 673 (2010), arXiv:1004.1856 [astro-ph.CO].
- [3] W. L. Freedman *et al.* (HST), *Astrophys. J.* **553**, 47 (2001), arXiv:astro-ph/0012376.
- [4] A. G. Riess *et al.* (Supernova Search Team), *Astron. J.* **116**, 1009 (1998), arXiv:astro-ph/9805201.
- [5] S. Perlmutter *et al.* (Supernova Cosmology Project), *Astrophys. J.* **517**, 565 (1999), arXiv:astro-ph/9812133.
- [6] A. G. Riess *et al.*, *Astrophys. J.* **826**, 56 (2016), arXiv:1604.01424 [astro-ph.CO].
- [7] A. G. Riess, S. Casertano, W. Yuan, J. B. Bowers,

- L. Macri, J. C. Zinn, and D. Scolnic, *Astrophys. J. Lett.* **908**, L6 (2021), arXiv:2012.08534 [astro-ph.CO].
- [8] J. Dunkley *et al.*, *Astrophys. J.* **739**, 52 (2011), arXiv:1009.0866 [astro-ph.CO].
- [9] P. A. R. Ade *et al.* (Planck), *Astron. Astrophys.* **571**, A16 (2014), arXiv:1303.5076 [astro-ph.CO].
- [10] P. A. R. Ade *et al.* (POLARBEAR), *Phys. Rev. Lett.* **113**, 021301 (2014), arXiv:1312.6646 [astro-ph.CO].
- [11] K. T. Story *et al.* (SPT), *Astrophys. J.* **810**, 50 (2015), arXiv:1412.4760 [astro-ph.CO].
- [12] P. A. R. Ade *et al.* (Planck), *Astron. Astrophys.* **594**, A13 (2016), arXiv:1502.01589 [astro-ph.CO].
- [13] S. Alam *et al.* (BOSS), *Mon. Not. Roy. Astron. Soc.* **470**, 2617 (2017), arXiv:1607.03155 [astro-ph.CO].
- [14] M. A. Troxel *et al.* (DES), *Phys. Rev. D* **98**, 043528 (2018), arXiv:1708.01538 [astro-ph.CO].
- [15] N. Aghanim *et al.* (Planck), *Astron. Astrophys.* **641**, A6 (2020), arXiv:1807.06209 [astro-ph.CO].
- [16] E. Di Valentino, *Nature Astron.* **1**, 569 (2017), arXiv:1709.04046 [physics.pop-ph].
- [17] E. Di Valentino *et al.*, (2020), arXiv:2008.11284 [astro-ph.CO].
- [18] E. Di Valentino, O. Mena, S. Pan, L. Visinelli, W. Yang, A. Melchiorri, D. F. Mota, A. G. Riess, and J. Silk, (2021), arXiv:2103.01183 [astro-ph.CO].
- [19] L. Perivolaropoulos and F. Skara, (2021), arXiv:2105.05208 [astro-ph.CO].
- [20] M. Lucca, (2021), arXiv:2105.09249 [astro-ph.CO].
- [21] S. Capozziello and M. De Laurentis, *Phys. Rept.* **509**, 167 (2011), arXiv:1108.6266 [gr-qc].
- [22] P. Bull *et al.*, *Phys. Dark Univ.* **12**, 56 (2016), arXiv:1512.05356 [astro-ph.CO].
- [23] W. Yang, S. Pan, E. Di Valentino, R. C. Nunes, S. Vagnozzi, and D. F. Mota, *JCAP* **09**, 019 (2018), arXiv:1805.08252 [astro-ph.CO].
- [24] W. Yang, E. Di Valentino, S. Pan, Y. Wu, and J. Lu, *Mon. Not. Roy. Astron. Soc.* **501**, 5845 (2021), arXiv:2101.02168 [astro-ph.CO].
- [25] S. Vagnozzi, *Phys. Rev. D* **102**, 023518 (2020), arXiv:1907.07569 [astro-ph.CO].
- [26] Y. Wang, L. Pogosian, G.-B. Zhao, and A. Zucca, *Astrophys. J. Lett.* **869**, L8 (2018), arXiv:1807.03772 [astro-ph.CO].
- [27] M. Reyes and C. Escamilla-Rivera, (2021), arXiv:2104.04484 [astro-ph.CO].
- [28] E. Colgáin, M. M. Sheikh-Jabbari, and L. Yin, (2021), arXiv:2104.01930 [astro-ph.CO].
- [29] V. Poulin, T. L. Smith, T. Karwal, and M. Kamionkowski, *Phys. Rev. Lett.* **122**, 221301 (2019), arXiv:1811.04083 [astro-ph.CO].
- [30] J. Sakstein and M. Trodden, *Phys. Rev. Lett.* **124**, 161301 (2020), arXiv:1911.11760 [astro-ph.CO].
- [31] S. X. Tian and Z.-H. Zhu, *Phys. Rev. D* **103**, 043518 (2021), arXiv:2102.06399 [gr-qc].
- [32] S. Nojiri, S. D. Odintsov, D. Saez-Chillon Gomez, and G. S. Sharov, (2021), arXiv:2103.05304 [gr-qc].
- [33] M. Chevallier and D. Polarski, *Int. J. Mod. Phys. D* **10**, 213 (2001), arXiv:gr-qc/0009008.
- [34] E. V. Linder and D. Huterer, *Phys. Rev. D* **72**, 043509 (2005), arXiv:astro-ph/0505330.
- [35] V. Barger, E. Guarnaccia, and D. Marfatia, *Phys. Lett. B* **635**, 61 (2006), arXiv:hep-ph/0512320.
- [36] E. Komatsu *et al.* (WMAP), *Astrophys. J. Suppl.* **180**, 330 (2009), arXiv:0803.0547 [astro-ph].

- [37] G. Cheng, Y.-Z. Ma, F. Wu, J. Zhang, and X. Chen, *Phys. Rev. D* **102**, 043517 (2020), arXiv:1911.04520 [astro-ph.CO].
- [38] C.-H. Chuang *et al.* (BOSS), *Mon. Not. Roy. Astron. Soc.* **471**, 2370 (2017), arXiv:1607.03151 [astro-ph.CO].
- [39] F. Beutler *et al.* (BOSS), *Mon. Not. Roy. Astron. Soc.* **464**, 3409 (2017), arXiv:1607.03149 [astro-ph.CO].
- [40] C. Blake *et al.*, *Mon. Not. Roy. Astron. Soc.* **425**, 405 (2012), arXiv:1204.3674 [astro-ph.CO].
- [41] G. C. Carvalho, A. Bernui, M. Benetti, J. C. Carvalho, and J. S. Alcaniz, *Phys. Rev. D* **93**, 023530 (2016), arXiv:1507.08972 [astro-ph.CO].
- [42] H.-J. Seo *et al.*, *Astrophys. J.* **761**, 13 (2012), arXiv:1201.2172 [astro-ph.CO].
- [43] S. Sridhar, Y.-S. Song, A. J. Ross, R. Zhou, J. A. Newman, C.-H. Chuang, F. Prada, R. Blum, E. Gaztañaga, and M. Landriau, *Astrophys. J.* **904**, 69 (2020), arXiv:2005.13126 [astro-ph.CO].
- [44] T. M. C. Abbott *et al.* (DES), *Mon. Not. Roy. Astron. Soc.* **483**, 4866 (2019), arXiv:1712.06209 [astro-ph.CO].
- [45] A. Tamone *et al.*, *Mon. Not. Roy. Astron. Soc.* **499**, 5527 (2020), arXiv:2007.09009 [astro-ph.CO].
- [46] F. Zhu *et al.*, *Mon. Not. Roy. Astron. Soc.* **480**, 1096 (2018), arXiv:1801.03038 [astro-ph.CO].
- [47] J. Hou *et al.*, *Mon. Not. Roy. Astron. Soc.* **500**, 1201 (2020), arXiv:2007.08998 [astro-ph.CO].
- [48] M. Blomqvist *et al.*, *Astron. Astrophys.* **629**, A86 (2019), arXiv:1904.03430 [astro-ph.CO].
- [49] H. du Mas des Bourboux *et al.*, *Astron. Astrophys.* **608**, A130 (2017), arXiv:1708.02225 [astro-ph.CO].
- [50] L. Chen, Q.-G. Huang, and K. Wang, *JCAP* **02**, 028 (2019), arXiv:1808.05724 [astro-ph.CO].
- [51] W. J. Handley, M. P. Hobson, and A. N. Lasenby, *Mon. Not. Roy. Astron. Soc.* **450**, L61 (2015), arXiv:1502.01856 [astro-ph.CO].
- [52] A. Lewis, (2019), arXiv:1910.13970 [astro-ph.IM].
- [53] L. Kazantzidis and L. Perivolaropoulos, *Phys. Rev. D* **97**, 103503 (2018), arXiv:1803.01337 [astro-ph.CO].
- [54] D. Benisty and D. Staicova, *Astron. Astrophys.* **647**, A38 (2021), arXiv:2009.10701 [astro-ph.CO].
- [55] H. Jeffreys, *The Theory of Probability*, Oxford Classic Texts in the Physical Sciences (1939).
- [56] S. Vagnozzi, A. Loeb, and M. Moresco, *Astrophys. J.* **908**, 84 (2021), arXiv:2011.11645 [astro-ph.CO].
- [57] S. Dhawan, J. Alsing, and S. Vagnozzi, (2021), arXiv:2104.02485 [astro-ph.CO].
- [58] G.-B. Zhao *et al.*, *Nature Astron.* **1**, 627 (2017), arXiv:1701.08165 [astro-ph.CO].
- [59] E. Di Valentino, A. Melchiorri, and J. Silk, *Astrophys. J. Lett.* **908**, L9 (2021), arXiv:2003.04935 [astro-ph.CO].
- [60] T. M. C. Abbott *et al.* (DES), *Phys. Rev. D* **99**, 123505 (2019), arXiv:1810.02499 [astro-ph.CO].
- [61] S. Lee *et al.* (DES), (2021), arXiv:2104.14515 [astro-ph.CO].

Complete Cornerplots

FIG. 3. The covariance test plot for the Λ CDM model.

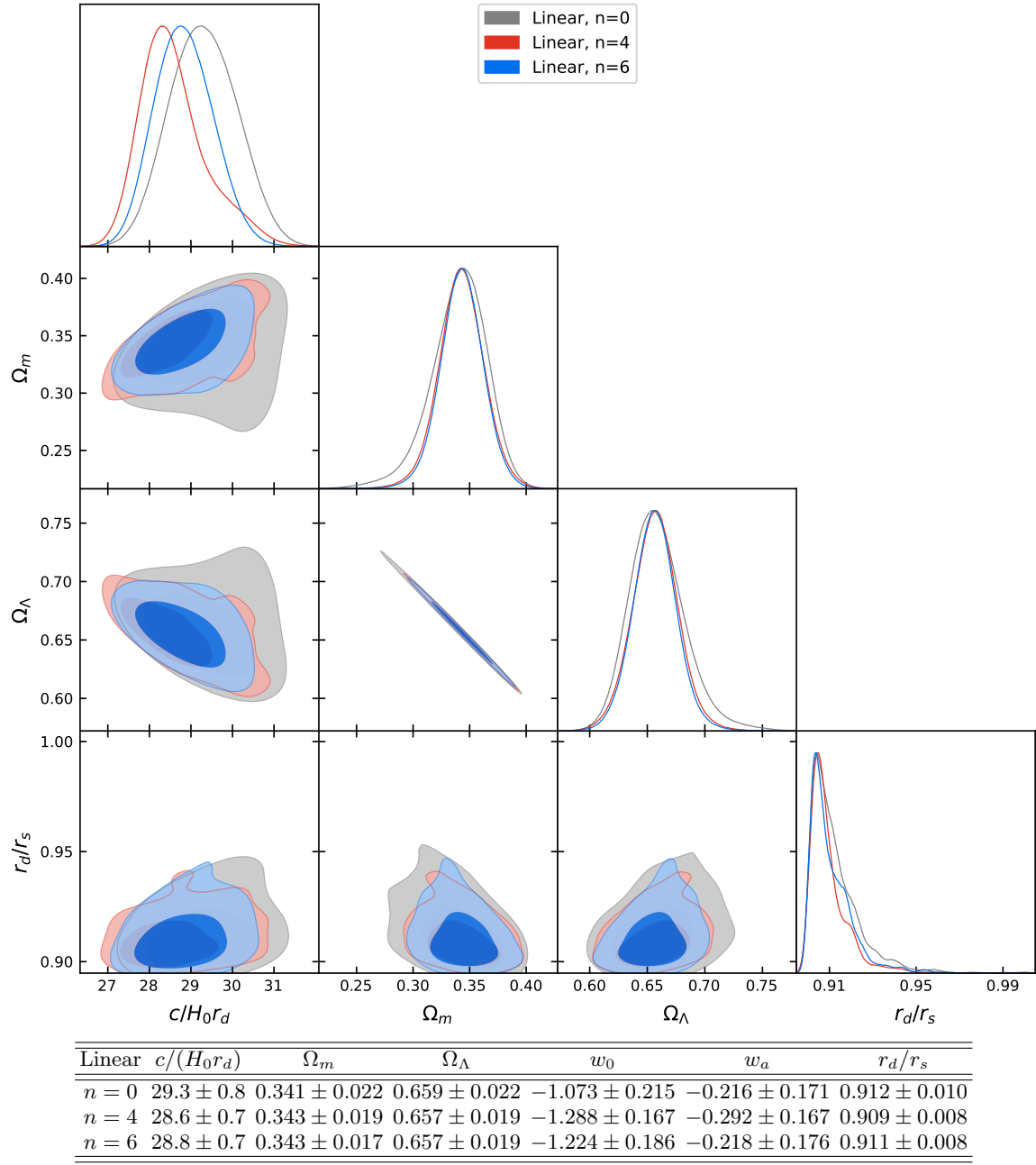


FIG. 4. The covariance test plot for the Linear model.

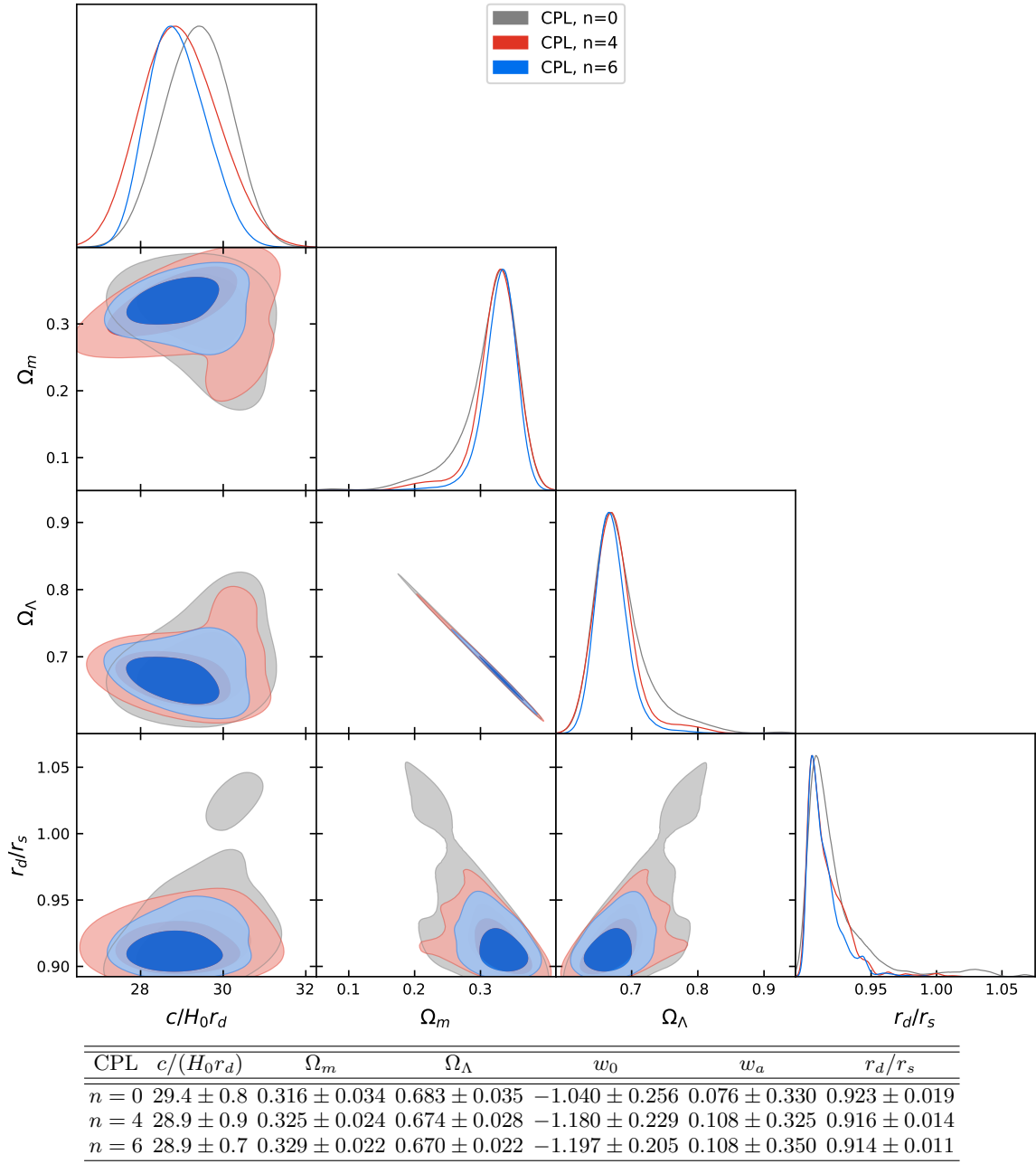


FIG. 5. The covariance test plot for the CPL model.

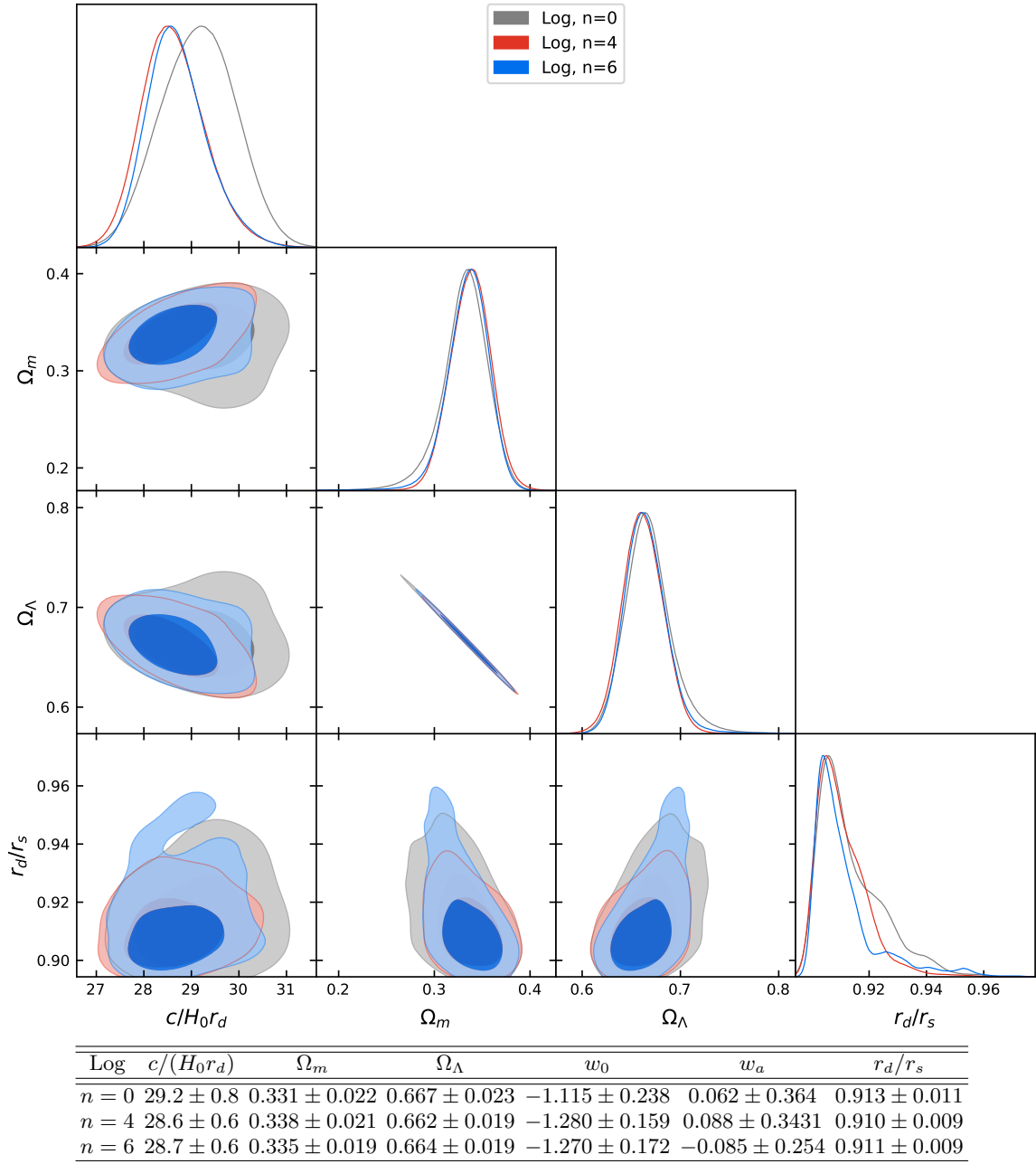
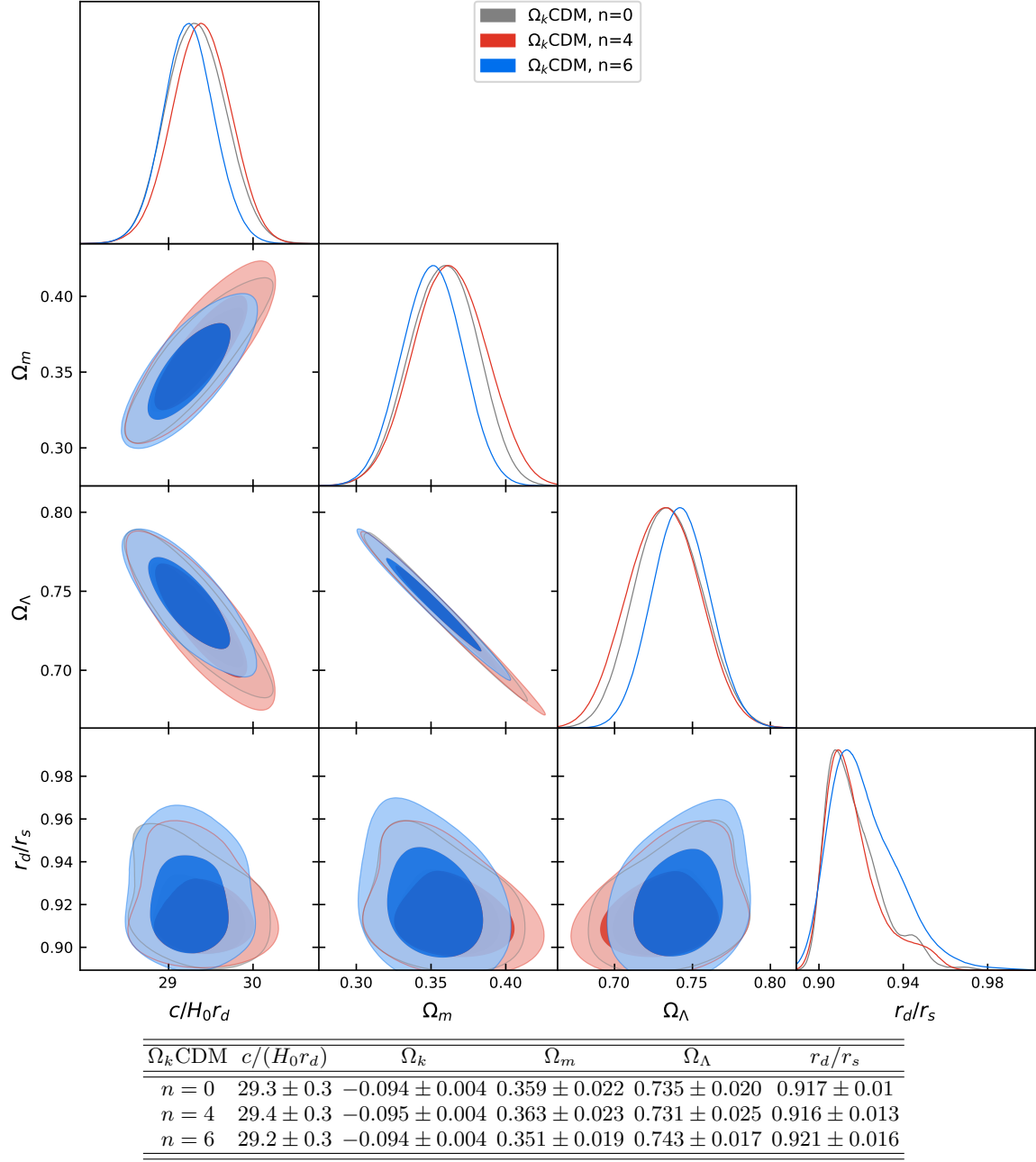


FIG. 6. The covariance test plot for the Log model.

FIG. 7. The covariance test plot for the $\Omega_k\Lambda CDM$ model.